

Ion-Induced Charge-Collection Transients in p-channel AlGaSb/InGaSb Field-Effect Transistors

Jeffrey H. Warner, Dale P. McMorow, *Member, IEEE*, Stephen Buchner, *Member, IEEE*, J. Brad Boos, Brian R. Bennett, Cory D. Cress, James G. Champlain, Nicolas Roche, *Member, IEEE*, Philippe Paillet, *Senior Member, IEEE*, Marc Gaillardin, *Member, IEEE*,

Abstract— The first ion-induced, time-resolved charge-collection measurements for p-channel AlGaSb/InGaSb field-effect transistors are reported. The transient response reveals two distinct decay regions; a fast initial decay (< 1 ns) followed by a slower decay (> 10 ns). The slow decay is associated with charge enhancement processes, which are explained by electron trapping and de-trapping via deep-level traps located in the AlGaSb barrier material. Charge enhancement effects are reported for different drain and gate bias conditions, and it is found that charge-enhancement effects are suppressed when the gate bias is increased toward depletion. The effects of the bias on the transient response are presented and discussed.

Index Terms— Single Event Transients, InAs, GaAs, AlGaSb, InGaSb, FET, HEMT, HFET, MESFET, heavy ions, protons, charge collection, SET cross section, charge enhancement, electron trapping, quantum well, Schottky barrier gate.

I. INTRODUCTION

Ultra high-speed, ultra low-power electronics are slated to play a key role in future-generation space and terrestrial systems. The III-V antimony (Sb) based compound semiconductors (ABCSs) are a leading contender to fill this high-speed, low-power need. This is because they have the highest electron and hole mobilities among III-V semiconductors and have significantly lower power consumption due to their much smaller bandgap [1]. Due to their unique material properties, antimony-based materials are of strong interest as the channel material for sub-0.5 Volt supply voltage, all-antimonide CMOS digital logic. With the novel advancements in the atomic layer deposition (ALD) of high- κ dielectric films on Sb-based materials, Penn State and Stanford research teams, in collaboration with the Naval Research Laboratory (NRL), have recently demonstrated Sb-based n-channel and p-channel metal-oxide-semiconductor quantum-well field-effect transistors (QWFETs), respectively [2, 3]. These new MOSFETs open the door to the development of an Sb-based complementary metal-oxide-

semiconductor (CMOS) technology that promises to dramatically lower the power dissipation in future high-speed logic circuits and extend Moore's Law [4].

From a radiation perspective, it is important to understand the fundamental mechanisms of charge-collection at the single transistor level. Only with an understanding of the basic carrier transport and collection mechanisms is it possible to develop effective mitigation approaches.

In this work we present ion-induced charge-collection transients measured for p-channel AlGaSb/InGaSb heterojunction FETs as a function of both drain and gate biases for MeV particle irradiation. Although SEEs have been investigated on n-channel FET technologies [5-8], this work represents the first measurements of the ion-induced single-event response of any p-channel Sb-based device.

II. EXPERIMENTAL DETAILS

The device used in this study is a depletion-mode heterojunction field-effect transistor (HFET) having a quantum well structure with a type I band alignment. The cross-section of the layer structure is shown in

Fig. 1. The equilibrium band diagram, which was calculated using NextNano simulation software [9], is given in Fig. 2. The p-type hole channel material is $\text{In}_{0.41}\text{Ga}_{0.59}\text{Sb}$ and the barrier material is $\text{Al}_{0.7}\text{Ga}_{0.3}\text{Sb}$. Hall measurements were performed on the channel material to determine the sheet conductivity and hole mobility which was found to be $1.4 \times 10^{12} \text{ cm}^{-2}$ and $1,170 \text{ cm}^2/\text{V-s}$, respectively. The HFETs are fabricated using alloyed source/drain ohmic contacts and a Schottky-barrier gate. The growth details of this structure are given in [10]. The device has a source-drain spacing of $3 \mu\text{m}$, a gate length of $0.2 \mu\text{m}$, and a gate width of $150 \mu\text{m}$. The current-voltage characteristics are shown in Fig. 3 and Fig. 4. The saturation threshold voltage for this device is 0.35 V .

The devices were irradiated at the Grand Accélérateur National d'Ions Lourds (GANIL, Caen, France) with a heavy ion broad beam using calcium ions with 238 MeV incident energy (5.92 MeV/amu); this corresponds to a linear energy transfer (LET) of $9.41 \text{ MeV cm}^2/\text{mg}$ in InGaSb and a range of approximately $40 \mu\text{m}$, calculated using the Monte Carlo based-code SRIM. The beam flux was $\sim 1.1 \times 10^6 \text{ ions/cm}^2/\text{sec}$ for all irradiations. At each bias condition, the device was exposed to an average fluence of $\sim 8 \times 10^8 \text{ ions/cm}^2$. The devices were irradiated in air at normal incidence and room temperature. During irradiation, the drain voltage was varied from -0.5 V to -1.5 V and the gate bias from 0 V to 0.6 V (depletion).

Manuscript received April 8, 2013. This work was supported by the Office of Naval Research and the Defense Threat Reduction Agency 6.1 basic research program.

J. H. Warner, D. McMorow, S. Buchner, J. B. Boos, Brian Bennett, Cory Cress, and James Champlain are with the Naval Research Laboratory, Washington DC 20375 USA (e-mail: Single-event-effects@nrl.navy.mil).

N. Roche, is a Post-Doctoral Fellow at the Naval Research Laboratory, Washington, DC 20375 USA.

P. Paillet and M. Gaillardin are with CEA, DAM, DIF, F-91297 ARPAJON, France.

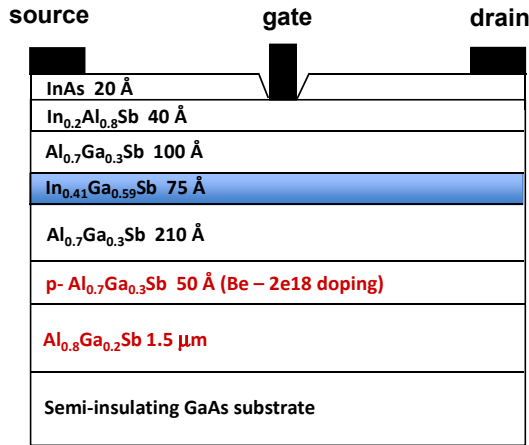


Fig. 1. Cross-section of an AlGaSb/InGaSb/AlGaSb p-channel FET.

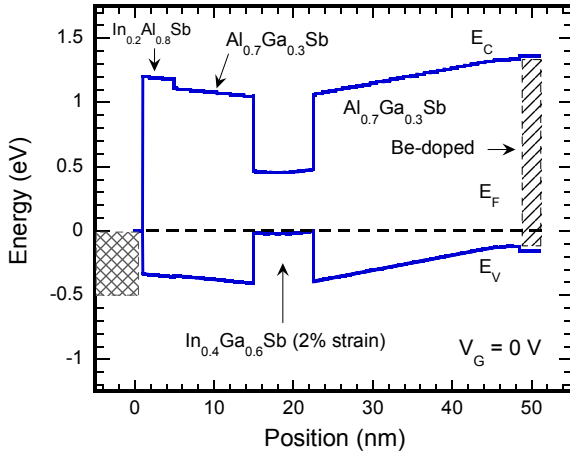
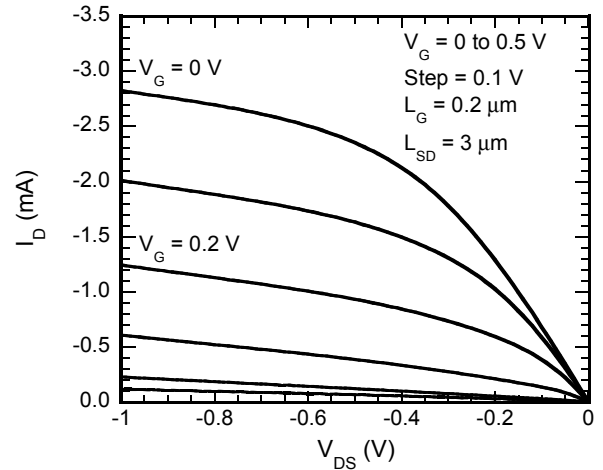
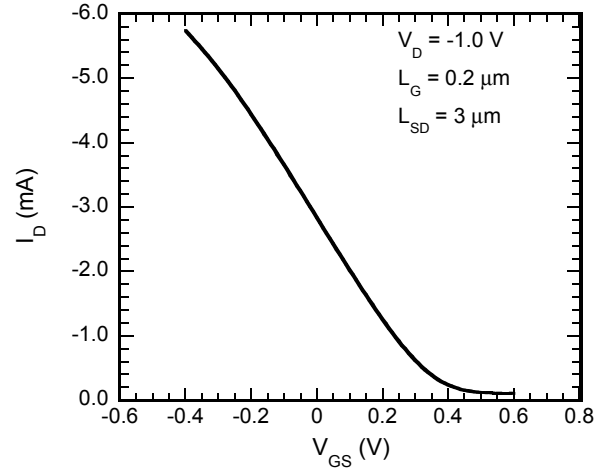


Fig. 2. Equilibrium band diagram for the structure shown in Fig. 1 which was simulated using NextNano [9].

The devices under test (DUT) are mounted in high-frequency (50 GHz) microwave packages with the gate and drain wire-bonded to microstrip transmission lines, and the source grounded. For the heavy ion measurements, the transient signals (gate and drain) are passed through a 26 GHz bias tee into the 50 ohm input of a Tektronix DPO71604B 16 GHz single shot oscilloscope connected via high frequency cables. The diagram of the experimental setup is shown in [8]. Each captured transient consists of 1,000 data points spanning a 20 ns temporal window, providing 20 ps resolution. The oscilloscope was set up to trigger and record drain transients. The trigger level was adjusted so that noise in the system did not trigger a measurement and this value was determined to be 2.4 mV. The average number of transients recorded during irradiation for a specific set of bias conditions was ~ 500 .

III. RESULTS

Fig. 5a shows a representative sampling (8 events) of drain transients measured for 238 MeV calcium ion irradiation with $V_D = -0.75$ V and $V_G = 0.2$ V. The transient response is comprised of three distinct regions; a very fast rise associated with the rapid collection of the deposited charge, followed by a decay that is well described by a double exponential function. Fig. 5b shows a comparison of a transient and an analytical fit (for $t > t_p$ where t_p is the time corresponding to

Fig. 3. Drain current (I_D) as a function of drain-source voltage (V_{DS}) for different gate bias conditions. The upper curve corresponds to a gate bias of 0 V, and the gate step was 0.1 V.Fig. 4. Drain current (I_D) as a function of gate-source voltage (V_{GS}) for a $V_{DS} = -1$ V. The saturation threshold voltage V_T is 0.35 V.

the peak of the transient) assuming the transient response follows a double exponential decay. The initial decay exhibits a time constant < 1 ns, while the slower decay has a time constant > 25 ns, and the data are well described by the fitted curve. Fig. 6a shows a representative sampling (8 events) of drain transients measured for 238 MeV calcium ion irradiation with $V_D = -0.75$ V and $V_G = 0.6$ V. In most cases, the slowly-relaxing tail is suppressed when the gate bias is increased to a value corresponding to a depletion condition. The constant τ_2 has been significantly reduced corresponding to a much faster decay time, which is clearly illustrated in Fig. 6b.

Fig. 7 shows the distribution of integral collected charge for (a) $V_G = 0.2$ V, and (b) $V_G = 0.6$ V with $V_D = -0.75$ V. The integral collected charge is determined by converting the voltage signal to a current by dividing by the 50 ohm input impedance of the oscilloscope and integrating to find the collected charge. The peak of the distribution shifts to much lower values of collected charge when the device is biased toward depletion, i.e. gate bias changed from 0.2 V to 0.6 V. The peak shifts from approximately 0.32 pC to 0.02 pC. At a given gate bias condition, there is a variation in transient

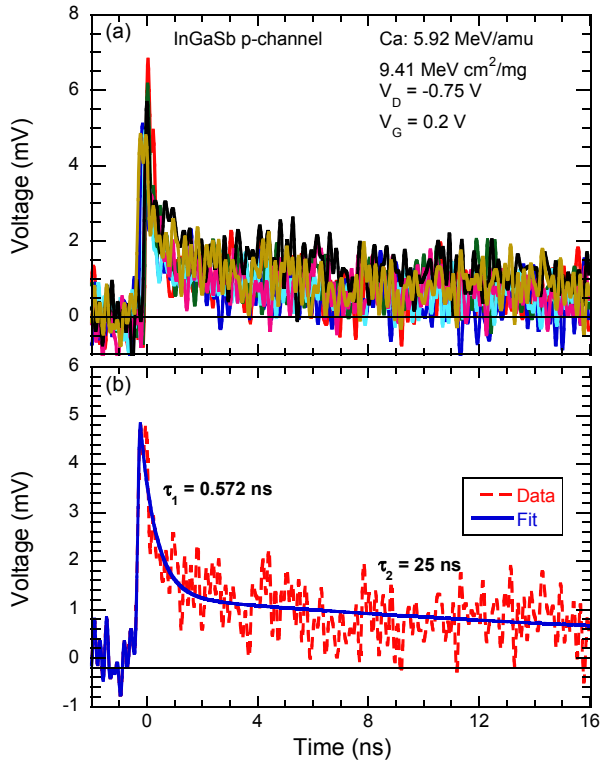


Fig. 5. (a) A comparison of several drain transients randomly selected from a population of ~ 400 transients that were recorded during 238 MeV calcium ion irradiation; $V_{DS} = -0.75$ V, $V_{GS} = 0.2$ V, and (b) an analytical fit (solid line) assuming the transient response follows a double exponential decay.

amplitude and shape (manifested in the collected charge values) which is associated with variation in ion strike location on the device. These variations, and the influence of gate bias on the transient response, can be more clearly illustrated with the data displayed in a dot plot format, as is shown in Fig. 8. The drain bias condition was $V_D = -0.75$ V. The data for each gate bias condition illustrates the range of values for the collected charge, full-width-half-maximum (FWHM), and transient amplitude. The solid lines in the figure correspond to the mean value at each gate bias condition. As the gate bias is increased from 0.2 V (accumulation bias condition) to 0.6 V (depletion bias condition), both the maximum and mean collected charge values decrease, the FWHM slightly decreases and the peak amplitude of the transient slightly increases. If the maximum or mean values are considered, as the gate bias is increased toward depletion, the transients become a little narrower at the FWHM and the amplitude slightly increases. These effects alone cannot account for the strong dependence of the collected charge with gate bias.

Fig. 9 illustrates the gate bias dependence on the data, using the fitted results to more clearly illustrate trends. For this figure, the individual transients represent the transient event corresponding to the maximum (worst-case) collected charge for each gate bias. It is evident that the slowly-relaxing tail, which contributes significantly to the integral collected charge, is suppressed as the gate bias is increased toward depletion. The FWHM parameter does not capture this behavior. A similar slow decay tail has been observed in

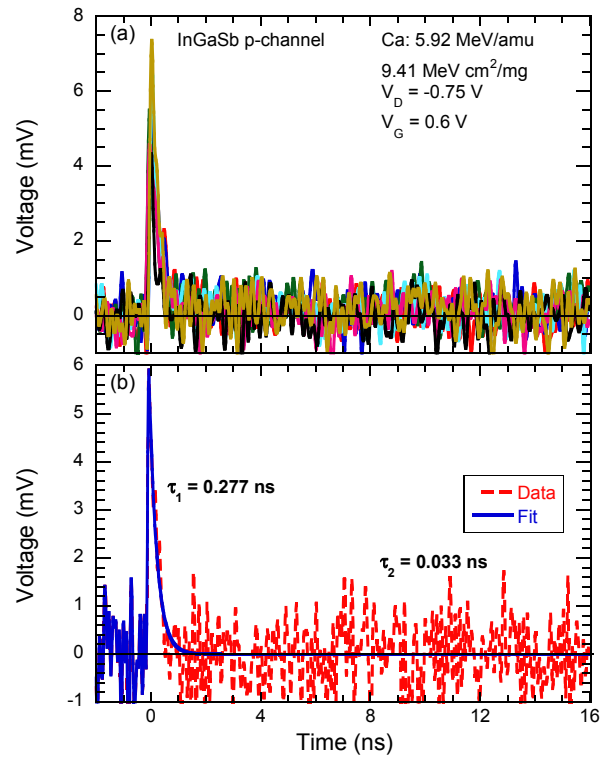


Fig. 6. (a) A comparison of several drain transients randomly selected from a population of ~ 450 transient that were recorded during 238 MeV calcium ion irradiation; $V_{DS} = -0.75$ V, $V_{GS} = 0.6$ V, and (b) an analytical fit (solid line) assuming the transient response follows a double exponential decay.

other III-V technologies, which has been attributed to charge enhancement mechanisms [6, 7, 11, 12]. Charge enhancement refers to the condition where the total integrated charge collected exceeds that deposited by the incident ion.

To determine if charge enhancement is evident in these devices, the total deposited charge (Q_{Dep}) can be calculated using the following equation:

$$Q_{Dep} = \frac{LET \cdot d \cdot \rho \cdot q}{E_{eh}}$$

where d is the thickness of the material, ρ is the material density, q is the charge of an electron, and E_{eh} is the electron-hole pair creation energy (3.125 eV for $In_{0.41}Ga_{0.59}Sb$ and 4.376 eV for $Al_{0.7}Ga_{0.3}Sb$). Most of the charge deposited in the $In_{0.41}Ga_{0.59}Sb$ channel layer is collected, but it is uncertain how much of a role the barrier material contributes to the collected charge. For this reason, the deposited charge was calculated to be 0.289 pC assuming all the epilayers contribute. This is an overestimation because not all the charge deposited in all the layers will be collected, plus this assumes a 100% collection efficiency. However, for a first approximation, this is a valid assumption. The maximum (worst-case) integral collected charge as a function of gate bias is shown in Fig. 10. The dashed line represents the calculated total deposited charge. The data shows that for gate biases less than 0.5 V, the collected charge is significantly higher than the deposited charge clearly indicating the presence of a charge enhancement effect.

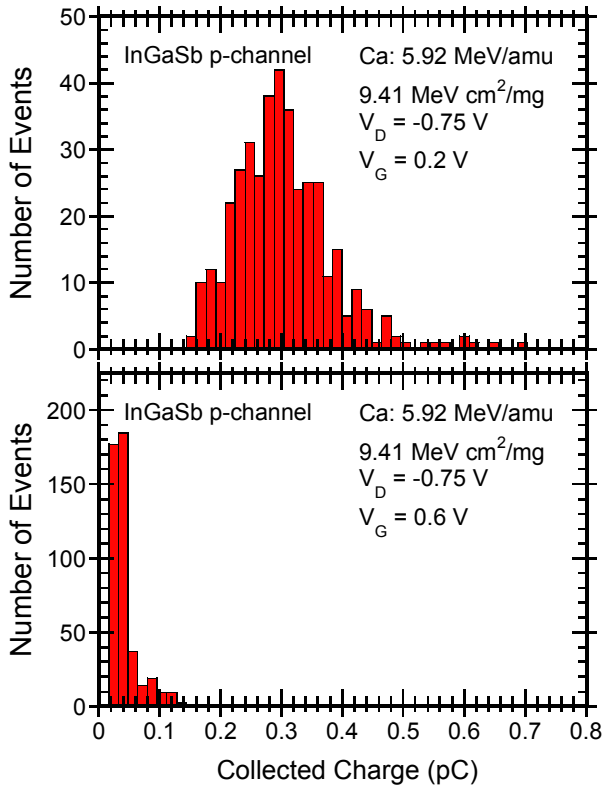


Fig. 7. Histogram showing the distribution of integral collected charge for $V_{DS} = -0.75$ V, and (a) $V_{GS} = 0.2$ V, (b) $V_{GS} = 0.6$ V. The device was irradiated with 238 MeV calcium ion irradiation.

The primary charge collection mechanism in these devices is the direct collection of charge deposited in the channel which gives the fast rise of the initial peak of the transient event. This process dominates when the channel is relatively depleted of carriers. In a previous study on n-channel Sb-based FETs, charge enhancement resulting from hole-accumulation/hole-trapping induced gate barrier lowering [13]. The type II band alignment in these devices facilitated this process by introducing a valence band offset between the buffer and the channel layers preventing collection of holes in the channel. In the current study, the device has a type I band alignment (c.f. Fig. 2, Fig. 11) and hole accumulation cannot explain the mechanism leading to charge enhancement. The excess holes generated in the AlGaSb barrier layer above the channel will be pushed toward the channel promoting hole collection, while the excess holes generated in the AlGaSb barrier layer beneath the channel will drift away from the channel. Furthermore, hole trapping in either barrier would deplete the channel further, thereby increasing the gate barrier.

Rather than hole accumulation in the buffer layer, the mechanism we observe here can be described by electron trapping in deep levels in the AlGaSb barrier layers. There has been evidence of deep traps in AlGaSb that we believe is the cause of charge enhancement [14, 15]. The trapped electrons can screen (modulate) the vertical gate field effectively lowering the gate potential barrier. The lowering of the gate potential barrier allows additional charge to flow from the source to the drain leading to charge enhancement. This process is discussed in more detail below.

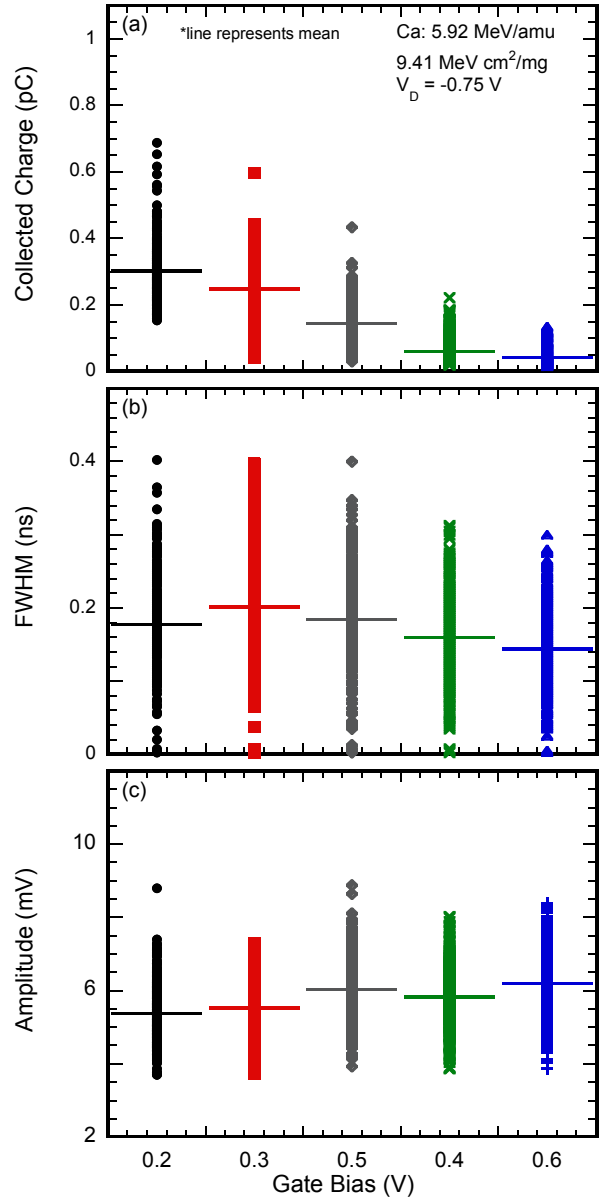


Fig. 8. Dot plot illustrating the gate bias dependence for three parameters characterizing an ion-induced transient; (a) collected charge, (b) full-width-half-maximum (FWHM), and (c) amplitude. These data correspond to a drain bias of $V_{DS} = -0.75$ V during irradiation.

The band structure in Fig. 11 illustrates the location of generated charge (electrons and holes represented by solid and open circles, respectively) after an ion strike and how the location of electron deep level defect states (thick dashed line) shift with respect to the Fermi level for a gate biases of: (a) $V_{GS} = 0.2$ V, and (b) $V_{GS} = 0.6$ V. After an ion strike, charge carriers (green circles) created in the In_{0.49}Ga_{0.51}Sb channel region are swiftly collected at the source-drain contacts. The rapid collection of these carriers in the channel results in the initial peak of the transient, and the peak amplitude of the transient has a slight increase with increasing gate bias (cf. Fig. 8c) because direct collection of charge carriers is dominate in depletion bias condition. Concurrently, excess electrons generated in the AlGaSb barrier layers, both above

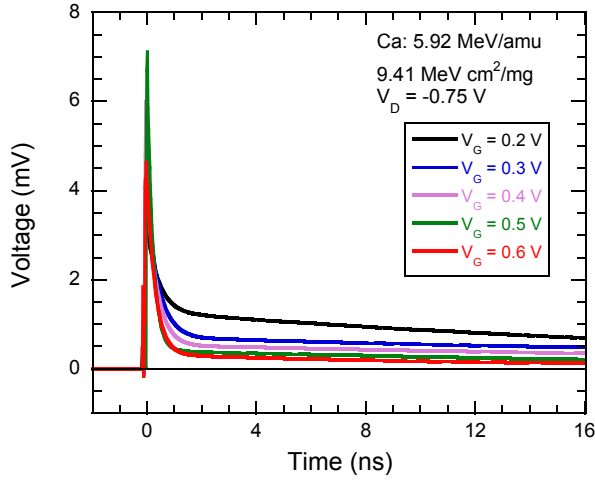


Fig. 9. This figure illustrates the gate bias dependence on the shape of the transients. Each transient corresponds to the maximum collected charge event at a given gate bias. These transients are an analytical fit to the raw data assuming the response follows a double exponential decay.

and below the channel, are captured at deep level defect states, presumably located near midgap. As shown in Fig. 11a for $V_{GS} = 0.2$ V, the deep level states are located above the Fermi level in both barrier regions and are initially unoccupied prior to an ion strike. After the ion-strike, the excess electrons in the upper barrier will accumulate due to the conduction band offset and eventually become captured by the deep levels (as suggested by the downward arrows in the figures). A similar process is possible for the excess electrons in the bottom barrier, but some of these electrons can also be collected by the channel. Trapped electrons, both above and below the channel, will reduce the gate potential barrier, causing additional current to flow from the source to the drain; this additional current flow leads to enhanced charge collection. Next, electron emission (not shown in the figure) from these deep levels, causes a slow modulation of the gate potential barrier until the deep levels are unoccupied by electrons, and the system has relaxed back to its equilibrium state. This process gives rise to the long-lived transient decay. The dependence of charge enhancement (including decay rate and total collected charge) on V_{GS} may be attributed to the trap density (number of occupied defects) and location of the deep level defect states with respect to the Fermi level.

As the gate bias is increased toward depletion, these electron deep level states begin to drop below the Fermi level, as illustrated in Fig. 11b (indicated by red circles), meaning they become permanently occupied with electrons. These trapped electrons will still screen the gate electric field, which may be one of the reasons why the devices cannot be biased into full pinch-off. But since there is no electron emission from the deep traps located below the Fermi level, the slow decay tail is more suppressed at this bias condition because only electron emission from deep level defect states below the channel contribute to the transient decay tail. Therefore, in depletion, the density of trapped electrons above the Fermi level is reduced, and less effective in modulating the gate potential barrier. This is also coupled with the fact that in depletion ($V_{GS} = 0.6$ V), the gate bias is above the sub

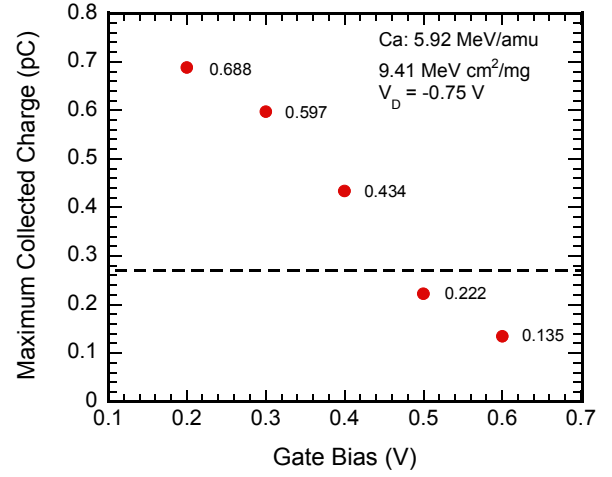


Fig. 10. Maximum collected charge as a function of gate bias for $V_{DS} = -0.75$ V. These data correspond to the maximum collected charge determined from the distribution of drain transients for each data set. The dashed line represented the deposited charge in all the epilayers.

threshold voltage ($V_{th} = 0.35$ V), so small modulations of the gate potential will have little effect on allowing additional current to flow from the source to the drain. The opposite is true when the gate is biased at 0.2 V. Small modulations of the gate potential can cause significantly current to flow as seen in Fig. 4.

Since charge enhancement depends on the density of filled electron states above the Fermi level, the location of the energy level within the bandgap will have a significant effect on charge enhancement.

IV. CONCLUSION

The results presented here provide a first examination of the single-event sensitivity of p-channel InGaSb FETs. The results are analogous to measurements performed on n-channel Sb-based transistor technology, however the charge enhancement mechanisms are of a different origin, with the bulk of the enhancement being associated with electron trapping and de-trapping of electrons in the AlGaSb barrier materials. These trapped electrons modulate the gate field, effectively lowering the gate potential barrier. The lowering of the gate potential barrier allows additional charge to flow from the source to the drain leading to enhanced source-drain (hole) current. These results provide a baseline for future studies as the technology evolves from the Schottky-barrier-gate devices of this study to the high- κ oxide III-V CMOS devices presently under development.

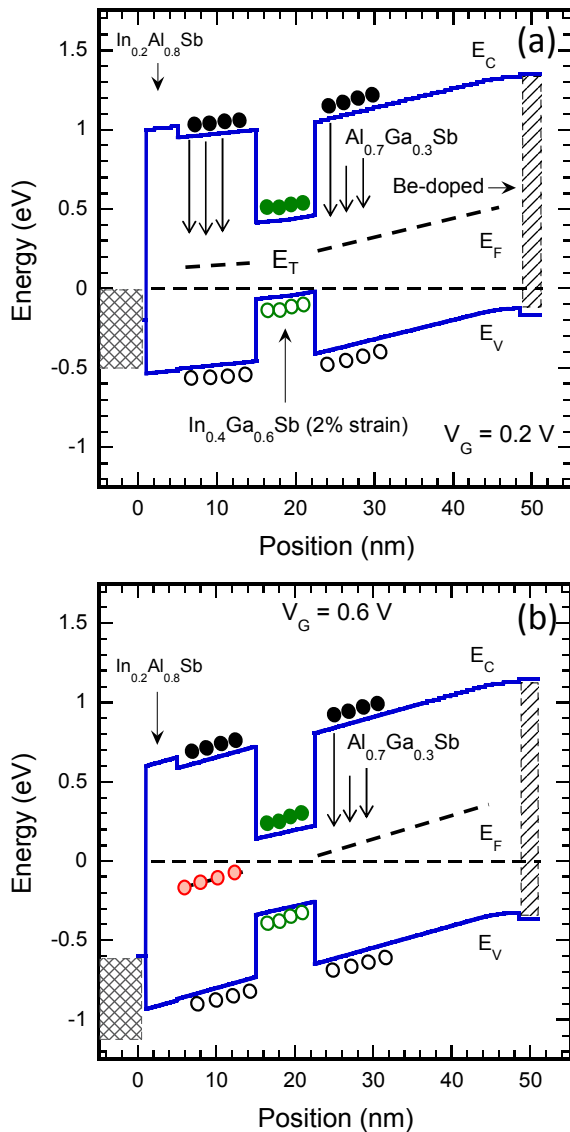


Fig. 11. Band diagram for different gate bias conditions: (a) $V_{GS} = 0.2$ V (accumulation), and (b) $V_{GS} = 0.6$ V (depletion). The solid circles represent electrons while the open circle represent holes that are created after an ion strike. The horizontal dashed line represents the Fermi level while the larger slanted dashed line represents an electron deep level defect located around midgap in the AlGaSb barrier material. The downward arrows indicate that after some time t after the ion strike, the electrons will populate the electron deep level defect.

REFERENCES

- [1] B. R. Bennett, R. Magno, J. B. Boos, W. Kruppa, and M. G. Ancona, "Antimonide-based compound semiconductors for electronic devices: A review," *Solid-State Electronics*, vol. 49, no. 12, pp. 1875-1895, 2005.
- [2] A. Ali, H. Madan, M. J. Barth, J. B. Boos, B. R. Bennett, and S. Datta, "Effect of Interface States on the Performance of Antimonide nMOSFETs," *IEEE Electron Device Letters*, vol. 34, no. 3, pp. 360-362, 2013.
- [3] A. Nainani, T. Irisawa, Y. Ze, B. R. Bennett, J. B. Boos, Y. Nishi, and K. C. Saraswat, "Optimization of the $Al_2O_3/GaSb$ Interface and a High-Mobility GaSb pMOSFET," *IEEE Transactions on Electron Devices*, vol. 58, no. 10, pp. 3407-3415, 2011.
- [4] R. Chau, S. Datta, M. Doczy, B. Doyle, B. Jin, J. Kavalieros, A. Majumdar, M. Metz, and M. Radosavljevic, "Benchmarking nanotechnology for high-performance and low-power logic transistor applications," *IEEE Transactions on Nanotechnology*, vol. 4, no. 2, pp. 153-158, 2005.
- [5] B. D. Weaver, J. B. Boos, N. A. Papanicolaou, B. R. Bennett, D. Park, and R. Bass, "High radiation tolerance of InAs/AlSb high-electron-mobility transistors," *Applied Physics Letters*, vol. 87, no. 17, pp. 173501, 2005.
- [6] D. McMorrow, J. B. Boos, A. R. Knudson, S. Buchner, Y. Ming-Jey, B. R. Bennett, and J. S. Melinger, "Charge-collection characteristics of low-power ultrahigh speed, metamorphic AlSb/InAs high-electron mobility transistors (HEMTs)," *IEEE Transactions on Nuclear Science*, vol. 47, no. 6, pp. 2662-2668, 2000.
- [7] D. McMorrow, J. B. Boos, A. R. Knudson, W. T. Lotshaw, P. Doe, J. S. Melinger, B. R. Bennett, A. Torres, V. Ferlet-Cavrois, J. E. Sauvestre, C. D'Hose, and O. Flament, "Transient response of III-V field-effect transistors to heavy-ion irradiation," *IEEE Transactions on Nuclear Science*, vol. 51, no. 6, pp. 3324-3331, 2004.
- [8] D. McMorrow, J. Warner, S. DasGupta, V. Ramachandran, J. B. Boos, R. Reed, R. Schrimpf, P. Paillet, V. Ferlet-Cavrois, J. Baggio, S. Buchner, F. El-Mamouni, M. Raine, and O. Duhamel, "Novel Energy-Dependent Effects Revealed in GeV Heavy-Ion-Induced Transient Measurements of Antimony-Based III-V HEMTs," *IEEE Transactions on Nuclear Science*, vol. 57, no. 6, pp. 3358-3365, 2010.
- [9] S. Birner, T. Zibold, T. Andlauer, T. Kubis, M. Sabathil, A. Trellakis, and P. Vogl, "nextnano: General Purpose 3-D Simulations," *IEEE Transactions on Electron Devices*, vol. 54, no. 9, pp. 2137-2142, 2007.
- [10] B. R. Bennett, M. G. Ancona, J. B. Boos, and B. V. Shanabrook, "Mobility enhancement in strained p-InGaSb quantum wells," *Applied Physics Letters*, vol. 91, no. 4, pp. 042104, 2007.
- [11] S. DasGupta, D. McMorrow, R. A. Reed, R. D. Schrimpf, and J. B. Boos, "Gate Bias Dependence of Single Event Charge Collection in AlSb/InAs HEMTs," *IEEE Transactions on Nuclear Science*, vol. 57, no. 4, pp. 1856-1860, 2010.
- [12] D. McMorrow, A. R. Knudson, J. B. Boos, P. Doe, and J. S. Melinger, "Ionization-induced carrier transport in InAlAs/InGaAs high electron mobility transistors," *IEEE Transactions on Nuclear Science*, vol. 51, no. 5, pp. 2857-2864, 2004.
- [13] V. Ramachandran, R. A. Reed, R. D. Schrimpf, D. McMorrow, J. B. Boos, M. P. King, G. Vizkelethy, X. Shen, and S. T. Pantelides, "Single-Event Transient Sensitivity of In-AlSb/InAs/AlGaSb High Electron Mobility Transistors," *IEEE Transactions on Nuclear Science*, vol. 59, no. 6, pp. 2691-2696, 2012.
- [14] W. Kruppa, J. B. Boos, B. R. Bennett, and B. P. Tinkham, "Low-Frequency Noise Characteristics of AlSb/InAsSb HEMTs," *Solid State Electronics*, vol. 48, pp. 2079-2084, 2004.

- [15] Y. Zhu, Y. Takeda, and A. Sasaki, "DX-center-like traps and persistent photoconductivity in Te-doped $\text{Al}_x\text{Ga}_{1-x}\text{Sb}$ on GaSb," *Journal of Applied Physics*, vol. 64, no. 4, pp. 1897-1901, 1988.